

# A variational data assimilation system for the range dependent acoustic model using the representer method: Theoretical derivations

Hans Ngodock,<sup>1,a)</sup> Matthew Carrier,<sup>1</sup> Josette Fabre,<sup>2</sup> Robert Zingarelli,<sup>2</sup> and Innocent Souopgui<sup>3</sup>

<sup>1</sup>The Naval Research Laboratory Code 7320, 1009 Balch Boulevard, Stennis Space Center, Mississippi 39529, USA

<sup>2</sup>The Naval Research Laboratory Code 7180, 1005 Balch Boulevard, Stennis Space Center, Mississippi 39529, USA

<sup>3</sup>Department of Marine Sciences, The University of Southern Mississippi, 1020 Balch Boulevard, Stennis Space Center, Mississippi 39529, USA

(Received 30 December 2016; revised 31 May 2017; accepted 8 June 2017; published online 13 July 2017)

This study presents the theoretical framework for variational data assimilation of acoustic pressure observations into an acoustic propagation model, namely, the range dependent acoustic model (RAM). RAM uses the split-step Padé algorithm to solve the parabolic equation. The assimilation consists of minimizing a weighted least squares cost function that includes discrepancies between the model solution and the observations. The minimization process, which uses the principle of variations, requires the derivation of the tangent linear and adjoint models of the RAM. The mathematical derivations are presented here, and, for the sake of brevity, a companion study presents the numerical implementation and results from the assimilation simulated acoustic pressure observations. [<http://dx.doi.org/10.1121/1.4989541>]

[JFL]

Pages: 186–194

## I. INTRODUCTION

Acoustic predictions are frequently made using estimates of the ocean that are modeled and constrained with oceanographic measurements (Helber *et al.*, 2008). Occasionally acoustic measurements are also made and are compared to such predictions (Colosi *et al.*, 1994; Colosi *et al.*, 1999). Acoustic models are sensitive to the ocean medium on scales as short as a fraction of a wavelength of interest, which is on the order of meters or fractions of meters (e.g.,  $\lambda \sim 3$  m for 500 Hz; Castor *et al.*, 2004; Lam *et al.*, 2009). Ocean model output scales are on the order of kilometers, and it is known that phenomena exist that can impact the acoustics at scales less than kilometers. For example, sound speed computed from data collected by a glider in the Western Pacific Ocean in 2007 (Fabre *et al.*, 2008) and corresponding sound speed computed from the Navy Coastal Ocean Model (NCOM; Martin, 2000) are shown in Fig. 1.

It is evident that there are ocean phenomena occurring at scales that are not captured by the model (NCOM) estimate. Acoustic transmission paths are determined by refractive indices, which are directly related to sound speed gradients. Both environments shown here contain a sonic layer or duct, which traps acoustic energy at certain frequencies (wavelengths) due to the upward refracting sound speed profiles near the surface. The duct is evident by the low loss

(high energy) of sound in the top  $\sim 50$  m shown in the 800 Hz range dependent acoustic model (RAM) transmission loss (TL) estimates in Fig. 2.

The glider data indicate that the duct is stronger than that estimated from NCOM. This is emphasized in Fig. 3, which shows TL estimated using the glider sound speed data at a receiver depth of 15 m. The differences in the structure of sound speed gradients that define the duct significantly impact the TL, resulting in a difference of more than 20 dB in the acoustic estimates.

Note that sound speed is not usually directly measured in the ocean; it is derived from the modeled or observed temperature and salinity (T/S) through algorithms such as the Chen-Millero-Li (Chen and Millero, 1977; Millero and Li, 1994) algorithm, see also Leroy *et al.* (2008). The differences between the observed and modeled sound speed can be reduced by assimilating the ocean T/S observations into the ocean model. However, this process may smooth out the acoustically significant features, primarily due to the coarse resolution often used in ocean models. Accurate acoustic prediction can significantly benefit from the ability to assimilate acoustic observations, which may consist of TLs, travel times, or acoustic pressure. By assimilating acoustic data into the acoustic model, not only is a more accurate prediction of the TL available, but also, an update to the oceanography that preserves the acoustically important characteristics of the waveguide can be inferred. In the first part of this study, we present the theory of acoustic data assimilation using variational analysis for updating an acoustic pressure prediction; the second part of the study presents the

<sup>a)</sup>Electronic mail: Hans.Ngodock@nrlssc.navy.mil

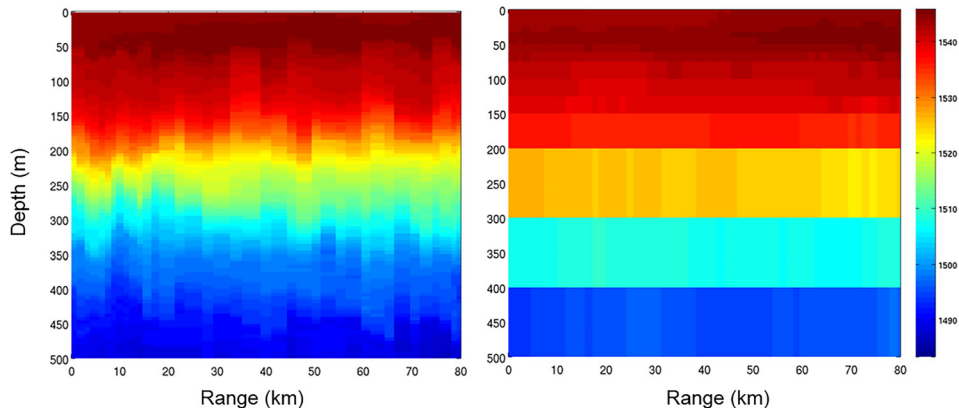


FIG. 1. (Color online) Glider (left) and NCOM (right) sound speeds for an acoustic track.

application of this assimilation technique using simulated acoustic pressure observations. The ability to update the associated environment will be the focus of a subsequent study.

The use of variational methods for solving inverse problems in ocean acoustic propagation modeled by the parabolic equation (PE) was investigated in recent years. [Elisseeff et al. \(2002\)](#) and [Hursky et al. \(2004\)](#) applied adjoint modeling to an acoustic tomography inversion problem; [Hermann et al. \(2006\)](#) used an adjoint of a similar PE in a geoacoustic inversion problem involving uncertainties in the sound speed; [Badran et al. \(2008\)](#) used adjoint modeling in another geoacoustic inversion for the seabed characterization; [Le Gac et al. \(2004\)](#) used a variational approach for geoacoustic inversion using adjoint modeling of a PE approximation model with nonlocal impedance boundary conditions; [Thode \(2004\)](#) and [Thode and Kim \(2004\)](#) used the adjoint model to compute the derivatives of a waveguide field with respect to several parameters, including the sound speed, density, and frequency; [Charpentier and Roux \(2004\)](#) used the adjoint method for the inversion of mode and wavenumber in shallow waters; [Meyer and Hermann \(2005\)](#) used the adjoint method with an optimal control method of nonlocal boundaries applied to the wide-angle PE for inversion of the acoustic field and bottom properties; [Li et al. \(2014\)](#) used a variational method for the inversion of an internal wave-perturbed sound-speed field via acoustic data assimilation, in the presence of acoustic pressure and sound-speed observations.

In most of the studies mentioned previously, the primary focus was not the correction of the acoustic pressure field, but rather on the geoacoustic inversion, using observations that are primarily based on tomography. This study follows the works of [Hursky et al. \(2004\)](#) and [Li et al. \(2014\)](#) who assimilated acoustic pressure observation in very shallow water (90–120 m depth) and rather short ranges (2–10 km) and a single frequency of 100 Hz. We describe the theoretical development and application of the adjoint method for the assimilation of acoustic pressure observations using the highly accurate RAM (e.g., [Collins, 1989, 1994](#)). To our knowledge, this is the first time such effort is undertaken (i.e., the development of an adjoint model for RAM and its use to assimilate acoustic pressure observations). RAM is based on the split-step Padé algorithm for solving the PE ([Collins 1993, 1994](#)), which allows large range steps and is the most efficient PE algorithm that has been developed ([Collins et al., 1996](#)). Solving the PE model using the split-step Padé algorithm introduces a series of differential operator multiplications and inversions that complicates the derivation of the adjoint model. Because the adjoint model must correspond to the particular numerical model under consideration, the adjoint models derived for the non-Padé approximations cannot be applied for the Padé approximation.

## II. THE MODEL

RAM is derived from the reduced wave equation in cylindrical coordinates with a harmonic point source,

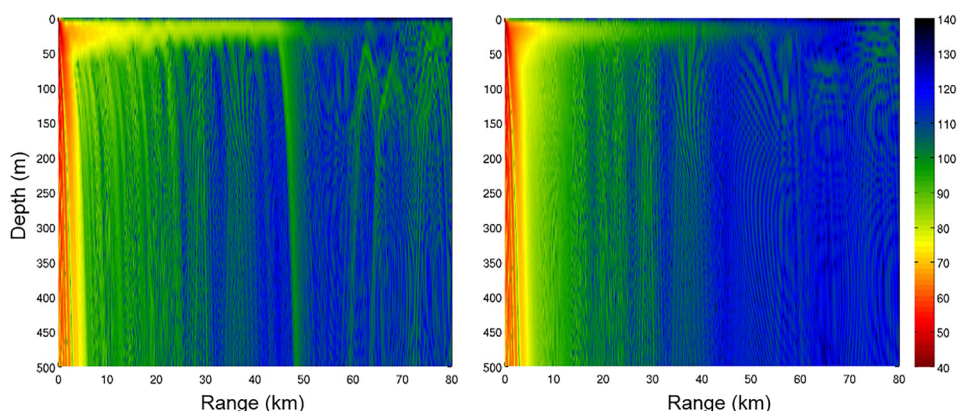


FIG. 2. (Color online) TL through environments shown in Fig. 1.

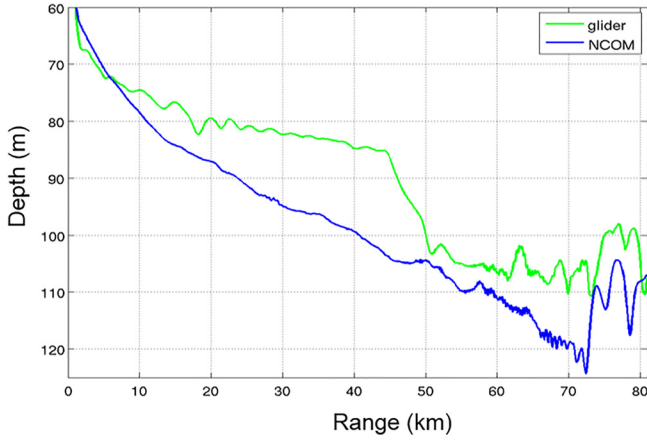


FIG. 3. (Color online) TLs at a receiver depth of 15 m for the glider (green) and NCOM (blue) data shown in Fig. 1.

removing the factor  $r^{-1/2}$  from the complex pressure  $p$  to handle cylindrical spreading, and assuming azimuthal symmetry to obtain (with a complex wavenumber to include attenuation)

$$\frac{\partial^2 p}{\partial r^2} + \rho \frac{\partial}{\partial z} \left( \frac{1}{\rho} \frac{\partial p}{\partial z} \right) + k^2 p = 0, \quad (1)$$

where  $k = (1 + i\eta\beta)(\omega/c(r, z))$  is the wavenumber,  $\omega$  is the angular frequency,  $c(r, z)$  is the speed of sound in range and depth,  $\beta$  is the attenuation coefficient, and  $\eta = (40\pi \log_{10} e)^{-1}$ . Factoring the operator in Eq. (1) yields

$$\left( \frac{\partial}{\partial r} + ik_0(I + X)^{1/2} \right) \left( \frac{\partial}{\partial r} - ik_0(I + X)^{1/2} \right) p = 0, \quad (2)$$

with

$$X = k_0^{-2} \left( \rho \frac{\partial}{\partial z} \frac{1}{\rho} \frac{\partial}{\partial z} + (k^2 - k_0^2) I \right), \quad (3)$$

where  $k_0 = \omega/c_0$ , and  $c_0$  is a representative phase speed. Assuming that outgoing energy dominates backscattered energy, Eq. (2) reduces to the outgoing wave equation

$$\frac{\partial p}{\partial r} = ik_0(I + X)^{1/2} p. \quad (4)$$

The formal solution of Eq. (4) is

$$p(r + \Delta r, z) = \exp(ik_0 \Delta r (I + X)^{1/2}) p(r, z), \quad (5)$$

where  $\Delta r$  is the range step. By applying an  $n$  term rational function to approximate the exponential, we have the Padé approximation

$$p(r + \Delta r, z) = \exp(ik_0 \Delta r) \prod_{i=1}^n \left( \frac{I + \alpha_{j,n} X}{I + \beta_{j,n} X} \right) p(r, z), \quad (6)$$

where  $I$  is the identity operator,  $\alpha_{j,n}$  and  $\beta_{j,n}$  are pre-computed coefficients of the split-step Padé algorithm for

solving the original wave equation implicitly by separation of variables. The product form in Eq. (6) can also be approximated, without loss of accuracy, by the summation form

$$p(r + \Delta r, z) = \exp(ik_0 \Delta r) \left( I + \sum_{j=1}^n \frac{\gamma_{j,n} X}{I + \beta_{j,n} X} \right) p(r, z), \quad (7)$$

as shown by Collins *et al.* (1996).

### III. THE ASSIMILATION SYSTEM

The assimilation system described in detail in Ngodock and Carrier (2014) for an ocean circulation model is adapted here for the acoustic propagation model. First, the model is cast in the following continuous form:

$$\begin{cases} \frac{\partial p}{\partial r} = F(p) + f, \\ p(r = 0, z) = I(z) + i(z), \end{cases} \quad (8)$$

where  $p$  is the acoustic pressure field,  $F$  includes the operators on the right-hand side of Eq. (6) or (7),  $f$  is the model error with covariance  $C_f$ ,  $I(z)$  is the prior initial condition (initial profile),  $i(z)$  is the initial condition error with covariance  $C_i$ , and  $z$  and  $r$  represent the position in a finite two-dimensional depth-range plane where  $0 \leq z \leq Z$  and  $0 \leq r \leq R$ . Consider a vector  $Y$  of  $M$  observations in the depth-range domain, with the associated vector of observation errors  $\varepsilon$  (with covariance  $C_\varepsilon$ ),

$$y_m = H_m p + \varepsilon_m, \quad 1 \leq m \leq M, \quad (9)$$

where  $H_m$  is the observation operator associated with the  $m$ th observation. The operator  $H$  transforms the model variables into observation equivalents. For the sake of simplicity, we assume that observations consist of direct measurements of the acoustic pressure, thus Eq. (9) takes the form  $y_m = p(r_m, z_m) + \varepsilon_m$ , where  $(r_m, z_m)$  denotes the position of the  $m$ th observation in the depth-range domain, and some spatial interpolation may have taken place. A weighted cost function is defined as

$$\begin{aligned} J = & \int_0^R \int_0^Z \int_0^R \int_0^Z f(r, z) W_f(r, z, r', z') f(r', z') dr' dz' dr dz \\ & + \int_0^Z \int_0^Z i(z) W_i(z, z') i(z') dz' dz + \varepsilon^T W_\varepsilon \varepsilon, \end{aligned} \quad (10)$$

where the weights  $W_f$  and  $W_i$  are defined as inverses of  $C_f$  and  $C_i$  in a convolution sense, and  $W_\varepsilon$  is the matrix inverse of  $C_\varepsilon$ . Boundary condition errors are omitted from Eqs. (8) and (10) only for the sake of clarity. The extrema of the cost function (10) can be found (Appendix A; see also Bennett, 2002) by solving the associated Euler-Lagrange (EL) system

$$\begin{cases} \frac{\partial p}{\partial r} = F(p) + C_f \cdot \lambda, \\ p(r=0) = I(z) + C_i \circ \lambda(0, z), \\ -\frac{\partial \lambda}{\partial r} = \left[ \frac{\partial F}{\partial p}(p) \right]^T \lambda - \sum_{m=1}^M \sum_{n=1}^M W_{\varepsilon, mn}(p(r_m, z_m) - y_m) \\ \quad \times \delta(r - r_n) \delta(z - z_n), \\ \lambda(R, z) = 0, \end{cases} \quad (11)$$

where  $\delta$  denotes the Dirac delta function,  $W_{\varepsilon, mn}$  are the matrix elements of  $W_\varepsilon$ , the superscript  $T$  denotes the transposition, and  $\lambda$  is the adjoint variable defined as the weighted residual

$$\lambda(r, z) = \int_0^R \int_0^Z W_f(r, z, r', z') f(r', z') dr' dz'. \quad (12)$$

The third and fourth equations in Eq. (11) are commonly called the adjoint model, and the multiplication of the covariance and the adjoint variable is the convolution

$$C_f \cdot \lambda(r, z) = \int_0^R \int_0^Z C_f(r, z, r', z') \lambda(r', z') dr' dz', \quad (13)$$

and

$$C_i \circ \lambda(0, z) = \int_0^Z C_i(z, z') \lambda(0, z') dz', \quad (14)$$

for the model and initial condition errors, respectively. The convolution involved in Eqs. (10)–(14) is written in a general form. However, the definition of the covariance functions as in Ngodock and Carrier (2014) gives this convolution its more familiar form. Also, the open and closed bullets represent the fact that the covariances are defined in the space of initial conditions ( $r=0$ ) and the entire range-depth space, respectively.

### A. The representer method

Allowing model errors and initial condition errors increases the dimension of the control space, the computational cost of the assimilation, and usually results in a poorly conditioned minimization process. This difficulty can be avoided if the minimization is done in the data space, which does not depend on, and is usually smaller than, the control space. That is possible through the representer algorithm, which is even more attractive in this case because of the scarcity of acoustic pressure observations (i.e., small observation space) and the linearity of Eqs. (4), (6), and (7) in terms of the acoustic pressure field. The representer method expresses the solution of the EL system (11) as the sum of a first guess and a finite linear combination of representer functions, one per datum. Thus, the representer method is the ideal choice for minimization of the cost function if acoustic pressure observations are available and one desires to correct only the acoustic pressure field, because the EL system (11) is linear in the acoustic pressure.

If, on the other hand, corrections to the sound speed and/or the attenuation coefficient are desired, then the EL system (11) becomes nonlinear, and the representer method cannot be applied to Eq. (11) directly. However, following Ngodock *et al.* (2000) and Bennett (2002), the representer algorithm can be applied to a linearized form of Eq. (11), obtained by either linearizing Eq. (11) directly or by linearizing the forward model Eqs. (4), (6), or (7) and deriving an EL associated with the cost function based on the linearized forward model. The iterative process by which the solution of the linearized EL becomes the background for the next linearization until formal convergence is known as the “outer loop,” whereas the “inner loop” consists of solving the linear EL system. In either case, given a background model solution  $p^0$  around which the model is linearized, one can write a linear EL system in the form

$$\begin{cases} \frac{\partial p^l}{\partial r} = F(p^{l-1}) + \left[ \frac{\partial F}{\partial p}(p^{l-1}) \right] (p^l - p^{l-1}) + C_f \cdot \lambda, \\ p^l(r=0) = I(z) + C_i \circ \lambda(0, z), \\ -\frac{\partial \lambda}{\partial r} = \left[ \frac{\partial F}{\partial p}(p^{l-1}) \right]^T \lambda - \sum_{m=1}^M \sum_{n=1}^M W_{\varepsilon, mn}(p^l(r_m, z_m) - y_m) \\ \quad \times \delta(r - r_n) \delta(z - z_n), \\ \lambda(R, z) = 0, \end{cases} \quad (15)$$

where  $l$  denotes the outer loop index,  $p^l$  is the EL solution after the  $l$ th outer loop. The EL system (15) is a linear coupled system between the adjoint and state variables. The representer method uncouples the system by expanding the solution as

$$p^l(r, z) = p_b^l(r, z) + \sum_{m=1}^M \gamma_m^l q_m^l(r, z), \quad (16)$$

where  $p_b^l$  is a first guess solution,  $\gamma_m^l$  are the coefficients and  $q_m^l(x, t)$ ,  $1 \leq m \leq M$ , are the representer functions defined by

$$\begin{cases} -\frac{\partial \mu_m^l}{\partial r} = \left[ \frac{\partial F}{\partial p}(p^{l-1}) \right]^T \mu_m^l - H^T \delta(r - r_m) \delta(z - z_m), \\ \mu_m^l(R) = 0, \\ \frac{\partial q_m^l}{\partial r} = F(p^{l-1}) + \left[ \frac{\partial F}{\partial p}(p^{l-1}) \right] q_m^l + C_f \cdot \mu_m^l, \\ q_m^l(r=0) = C_i \circ \mu_m^l(0, z). \end{cases} \quad (17)$$

Note that the equations in Eq. (17) are only weakly coupled, since the  $\mu_m^l$ , also known as the adjoint representer functions, depend only on the observation locations, and can be computed independently of the  $q_m^l$ . The adjoint equations in Eq. (16) or (17) are integrated backwards in range as indicated by the final conditions, and the first guess in Eq. (16) can be chosen as the previous outer loop solution  $p^{l-1}$ , or the tangent linear solution around  $p^{l-1}$ . It may be shown (e.g., Bennett, 2002) that the representer coefficients  $\gamma_m^k$  are computed by



solving a linear system in data space involving the representer matrix, the data error covariance matrix, and the innovation vector

$$(Q^l + C_\epsilon)\gamma^l = Y - Hp_b^l, \quad (18)$$

where  $Q^l$  is the representer matrix with elements  $Q_{mn}^k = q_m^k(r_n, z_n)$ , i.e., the  $m$ th representer function evaluated at the  $n$ th observation location  $(r_n, z_n)$ . The detailed derivation of Eq. (18) from Eqs. (16) and (17) is given in Appendix B. The entire representer matrix need not be computed explicitly since the linear system (18) can be solved using an iterative algorithm (e.g., the conjugate gradient), by taking advantage of the symmetry of each matrix. The representer coefficients constitute the right-hand side of the adjoint equation in the EL system. Thus, once the representer coefficients are computed, they are substituted into the adjoint equation, which is then solved and substituted in the forward linear equation to obtain the final solution. A background solution around which the model is linearized is required. Usually it is the solution of the nonlinear model. For the first guess solution, one may consider either the background or the tangent linear solution around the background. The new optimal solution may replace the background for another minimization process (i.e., outer loops) until formal convergence, as in Bennett *et al.* (1996, 1998, 2000) and Ngodock *et al.* (2000, 2007, 2009).

## B. Linearization

Although Eq. (4) is linear in the acoustic pressure  $p$ , it is nonlinear in the differential operator  $X$ , which depends nonlinearly on the wavenumber  $k$ . The latter is also a function of both the sound speed and the attenuation coefficient. This exacerbates the nonlinearity of both Eqs. (6) and (7). The following linearization is based on the first order Taylor's expansion. Small perturbations  $\tilde{c}$  and  $\tilde{\beta}$  on both the sound speed and the attenuation coefficient, respectively, result in a perturbation of the wavenumber that is given by

$$\tilde{k} = i\eta\tilde{\beta}\frac{\omega}{c(r, z)} - (1 + i\eta\beta)\frac{\tilde{c}(r, z)}{c^2(r, z)}, \quad (19)$$

which, in turn, generates a perturbation  $\tilde{X}$  of the differential operator  $X$  in Eq. (3) given by

$$\tilde{X} = 2k_0^{-2}k\tilde{k}I. \quad (20)$$

The linearization of the product form of the solution (6) becomes

$$\begin{aligned} \tilde{p}(r + \Delta r, z) &= \exp(ik_0\Delta r) \prod_{j=1}^n \left( \frac{I + \alpha_{j,n}X}{I + \beta_{j,n}X} \right) \tilde{p}(r, z) \\ &+ \exp(ik_0\Delta r) \sum_{j=1}^n \left( \prod_{\substack{l=1 \\ l \neq j}}^n \left( \frac{I + \alpha_{l,n}X}{I + \beta_{l,n}X} \right) \right) \\ &\times \left( \frac{\beta_{j,n} - \alpha_{j,n}}{(I + \beta_{j,n}X)^2} \right) \tilde{X}p(r, z) \end{aligned} \quad (21)$$

and the linearization of the summation form of the solution (7) is given by

$$\begin{aligned} \tilde{p}(r + \Delta r, z) &= \exp(ik_0\Delta r) \left( I + \sum_{j=1}^n \frac{\gamma_{j,n}X}{(I + \beta_{j,n}X)} \right) \tilde{p}(r, z) \\ &+ \exp(ik_0\Delta r) \sum_{j=1}^n \left( \frac{\gamma_{j,n}}{(I + \beta_{j,n}X)^2} \right) \tilde{X}p(r, z). \end{aligned} \quad (22)$$

Both Eqs. (21) and (22) describe the evolution of small perturbations  $\tilde{p}(r, z)$  of the acoustic pressure field as the result of the small perturbations applied to the sound speed and the attenuation coefficient, given a prior or background pressure field  $p(r, z)$  around which the model is linearized.

## C. The adjoint

We now derive the adjoint of both Eqs. (6) and (7). Note that the adjoint model in Eq. (15) is only different from the adjoint representer model in Eq. (17) by the forcing term: the former is forced by the weighted differences between the model and the observations (also called the innovations) at the observation locations, and the latter is only forced by Dirac delta functions centered at the observation locations. So, the forcing term of the adjoint in Eq. (15) is a linear combination of the forcing term of the adjoint in Eq. (17). Thus, due to the linearity of the adjoint model, it can be seen that the solution to the adjoint model in Eq. (15) is a linear combination of the adjoint representer solutions in Eq. (17), with coefficients that depend on the optimal solution  $p^l$ , which is yet to be determined. We can therefore derive the adjoint in Eq. (17) for the  $m$ th observation as it will carry less cumbersome terms on the right-hand side. We drop the superscripts  $k$  (of the outer loops) and subscripts  $m$  (except for the observation location) for brevity. Note that in addition to the adjoint variable  $\mu_p$ , associated with the acoustic pressure variable, there are also adjoint variables  $\mu_X$ ,  $\mu_k$ ,  $\mu_c$ , and  $\mu_\beta$ , associated with the differential operator  $X$ , the wavenumber  $k$ , the sound speed  $c$  and the attenuation coefficient  $\beta$ , respectively.

The adjoint model in Eq. (17) is initialized at  $r = R$  by

$$\mu_p(R, z) = H_m^T \delta(R - r_m) \delta(z - z_m). \quad (23)$$

Following Eq. (21), the adjoint of the product form (6) is

$$\begin{aligned} \mu_p(r, z) &= \exp(ik_0\Delta r) \prod_{j=1}^n \left( \frac{I + \alpha_{j,n}X}{I + \beta_{j,n}X} \right) \mu_p(r + \Delta r, z) \\ &+ H_m^T \delta(r - r_m) \delta(z - z_m), \end{aligned} \quad (24)$$

$$\begin{aligned} \mu_X &= \exp(ik_0\Delta r) \sum_{j=1}^n \left( \prod_{\substack{l=1 \\ l \neq j}}^n \left( \frac{I + \alpha_{l,n}X}{I + \beta_{l,n}X} \right) \right) \\ &\times \left( \frac{\beta_{j,n} - \alpha_{j,n}}{(I + \beta_{j,n}X)^2} \right) p(r, z) \mu_p(r + \Delta r, z). \end{aligned} \quad (25)$$

Similarly, following Eq. (22) the adjoint of the summation form (7) is

$$\mu_p(r, z) = \exp(ik_0\Delta r) \sum_{j=1}^n \left( \frac{\alpha_{j,n}X}{(I + \beta_{j,n}X)} \right) \mu_p(r, z + \Delta r) + H_m^T \delta(r - r_m) \delta(z - z_m), \quad (26)$$

$$\mu_X(r, z) = \exp(ik_0\Delta r) \sum_{j=1}^n \left( \frac{\alpha_{j,n}}{(I + \beta_{j,n}X)^2} \right) \times p(r, z) \mu_p(r, z + \Delta r). \quad (27)$$

Having computed  $\mu_X$  from either Eq. (25) or (27), we relate the adjoint acoustic information to the adjoint of the environmental variables using Eqs. (20) and (19),

$$\mu_k = \frac{2k}{k_0^2} I \mu_X, \quad (28)$$

$$\mu_\beta = i\eta \frac{w}{c} \mu_k, \quad (29)$$

$$\mu_c = -\frac{w}{c^2} \mu_k. \quad (30)$$

If the correction to the ocean environment is desired, then one would exploit the connection of the sound speed to the ocean temperature ( $T$ ) and salinity ( $S$ ) through the sound speed equation [e.g., Chen-Millero-Li (Chen and Millero, 1977; Millero and Li, 1994) algorithm]

$$c = F(T, S), \quad (31)$$

where  $F$  is usually a polynomial. The linearization of Eq. (31) is written as

$$\tilde{c} = \frac{\partial F}{\partial T} \tilde{T} + \frac{\partial F}{\partial S} \tilde{S}. \quad (32)$$

From Eqs. (31) and (32), the correction to the ocean T/S is obtained by

$$\mu_T = \left[ \frac{\partial F}{\partial T} \right]^T \mu_c, \quad (33)$$

and

$$\mu_S = \left[ \frac{\partial F}{\partial S} \right]^T \mu_c. \quad (34)$$

#### IV. SUMMARY

The theoretical framework for the development of a variational data assimilation system for the highly accurate RAM acoustic propagation model is presented. This development is adapted from methods developed for ocean circulation models (Ngodock and Carrier, 2014) using the representer method, and is applied to both the product and sum forms of the split-step Padé algorithm in RAM. Both tangent linear and adjoint models of RAM have been developed to allow acoustic pressure to be assimilated into RAM. The companion study consists of implementation and demonstration of these theoretical derivations, followed by numerical results that show the usefulness of the system.

#### ACKNOWLEDGMENTS

This work was sponsored by the Office of Naval Research Program Element 0601153N as part of the ‘‘Acoustic Data Assimilation for Remote Decision Applications’’ project. This paper is Navy Research Laboratory (NRL) Paper Contribution No. NRL/JA/7320-16-3234. The authors would like to thank the anonymous reviewers, whose comments helped to improve the quality of the manuscript.

#### APPENDIX A: DERIVATION OF THE EL SYSTEM

In this first part of the appendix we present the detailed derivation of the EL system (11) associated with the minimization of the cost function (10),

$$J = \int_0^R \int_0^Z \int_0^R \int_0^Z f(r, z) W_f(r, z, r', z') f(r', z') dr' dz' dr dz + \int_0^Z \int_0^Z i(z) W_i(z, z') i(z') dz' dz + \varepsilon^T W_\varepsilon \varepsilon. \quad (A1)$$

The cost function (A1) can be rewritten as

$$J = \int_0^R \int_0^Z \int_0^R \int_0^Z \left[ \frac{\partial p(r, z)}{\partial r} - F(p(r, z)) \right] W_f(r, z, r', z') \times \left[ \frac{\partial p(r', z')}{\partial r} - F(p(r', z')) \right] dr' dz' dr dz + \int_0^Z \int_0^Z (p(0, z) - I(z)) W_i(z, z') \times (p(0, z') - I(z')) dz' dz + \sum_{m=1}^M \sum_{n=1}^M (p(r_m, z_m) - y_m) \times W_{\varepsilon, mn} (p(x_n, t_n) - y_n) \quad (A2)$$

to make the dependence of  $J$  upon  $p$  explicit. The calculus of variations indicates that for  $p$  to be a local extremum of  $J$  we must have

$$\delta J = J[p + \delta p] - J[p] = O(\delta p)^2, \quad (A3)$$

for any small perturbation  $\delta p$ ,

$$\begin{aligned} \delta J &= J[p + \delta p] - J[p] \\ &= 2 \int_0^R \int_0^Z \int_0^R \int_0^Z \left[ \frac{\partial \delta p(r, z)}{\partial r} - \left[ \frac{\partial F}{\partial p}(p) \right] \delta p(r, z) \right] \\ &\quad \times W_f(r, z, r', z') \left[ \frac{\partial p(r', z')}{\partial r} - F(p(r', z')) \right] dr' dz' dr dz \\ &\quad + 2 \int_0^Z \int_0^Z (\delta p(0, z)) W_i(z, z') (p(0, z') - I(z')) dz' dz \\ &\quad + 2 \sum_{m=1}^M \sum_{n=1}^M (\delta p(r_m, z_m)) W_{\varepsilon, mn} (p(x_n, t_n) - y_n). \end{aligned} \quad (A4)$$

After conveniently introducing the weighted residual (12) and using some integration by parts, the first integral term in Eq. (A4) is

$$\begin{aligned}
& 2 \int_0^R \int_0^Z \lambda \left[ \frac{\partial \delta p}{\partial r} - \left[ \frac{\partial F}{\partial p}(p) \right] \delta p(r, z) \right] dz dr \\
&= 2 \int_0^R \int_0^Z \left[ -\frac{\partial \lambda}{\partial r} - \left[ \frac{\partial F}{\partial p}(p) \right]^T \lambda \right] \delta p(r, z) dz dr \\
&+ 2 \int_0^Z \lambda(R, z) \delta p(R, z) dz - 2 \int_0^Z \lambda(0, z) \delta p(0, z) dz.
\end{aligned} \tag{A5}$$

Also, the last term in Eq. (A4) can be rewritten as

$$\begin{aligned}
& 2 \sum_{m=1}^M \sum_{n=1}^M \delta p(r_m, z_m) W_{\varepsilon, mn} (p(r_n, z_n) - y_n) \\
&= 2 \int_0^R \int_0^Z \sum_{m=1}^M \sum_{n=1}^M \delta p(x, t) W_{\varepsilon, mn} (p(x_n, t_n) - y_n) \\
&\quad \times \delta(z - z_m) \delta(r - r_m) dz dr,
\end{aligned} \tag{A6}$$

where the second and third deltas in the right-hand side are Dirac delta functions. In the case of uncorrelated observation errors, i.e.,

$$W_{\varepsilon, mn} = \begin{cases} \sigma_m^{-2}, & \text{if } m = n \\ 0, & \text{if } m \neq n, \end{cases} \tag{A7}$$

as is often assumed in practice, where  $\sigma_m$  is the observation error standard deviation, Eq. (A6) becomes

$$\begin{aligned}
& 2 \sum_{m=1}^M \sum_{n=1}^M \delta p(r_m, z_m) W_{\varepsilon, mn} (p(r_n, z_n) - y_n) \\
&= 2 \int_0^R \int_0^Z \delta p(x, t) \sum_{m=1}^M W_{\varepsilon, mm} (p(x_m, t_m) - y_m) \\
&\quad \times \delta(z - z_m) \delta(r - r_m) dz dr.
\end{aligned} \tag{A8}$$

With this last rewriting, all terms in Eq. (A4) now depend explicitly and linearly on  $\delta p$ . Thus, for the local extremum condition (A3) to be satisfied, all the coefficients of  $\delta p(r, z)$ ,  $\delta p(0, z)$ , and  $\delta p(R, z)$  must vanish, i.e.,

$$\begin{cases} -\frac{\partial \lambda}{\partial t} - \left[ \frac{\partial F}{\partial p}(p) \right]^T \lambda + \sum_{m=1}^M \sigma_m^{-2} (p(r_m, z_m) - y_m) \\ \quad \times \delta(r - r_m) \delta(z - z_m) = 0, \\ \lambda(R, z) = 0, \\ -\lambda(0, z) + W_i [p(0, z) - I(z)] = 0. \end{cases} \tag{A9}$$

The equations in Eq. (A9) constitute the EL conditions for local extrema of the cost function. Recalling the definition of the weighted residual (12) and the inverse of the covariances, e.g.,  $\int_0^R \int_0^Z W_f(r, z, r', z') C_f(r', z', r'', z'') dz' dr' = \delta(r - r'') \delta(z - z'')$ , we can combine Eq. (A9) with the model (8) to get the EL system (11)

$$\begin{cases} \frac{\partial p}{\partial t} = F(p) + C_f \cdot \lambda(r, z), \\ p(0, z) = I(z) + C_i \circ \lambda(0, z), \\ -\frac{\partial \lambda}{\partial t} - \left[ \frac{\partial F}{\partial p}(p) \right]^T \lambda = -\sum_{m=1}^M \sigma_m^{-2} (p(r_m, z_m) - y_m) \\ \quad \times \delta(r - r_m) \delta(z - z_m), \\ \lambda(R, z) = 0. \end{cases}$$

## APPENDIX B: THE REPRESENTER METHOD

As stated in the manuscript, the linear expansion (16) can only be applied to a linearized form of the EL system. We describe below the detailed derivations that lead to the linear system (18) by first adopting the following linearization for Eq. (16):

$$\begin{cases} \frac{\partial \tilde{p}}{\partial r} = F \tilde{p} + G + C_f \cdot \lambda, \\ \tilde{p}(r=0) = I(z) + C_i \circ \lambda(0, z), \\ -\frac{\partial \lambda}{\partial r} = F^T \lambda - \sum_{m=1}^M W_{\varepsilon, mm} (\tilde{p}(r_m, z_m) - y_m) \\ \quad \times \delta(r - r_m) \delta(z - z_m), \\ \lambda(R, z) = 0, \end{cases} \tag{B1}$$

where  $F = [(\partial F / \partial p)(p)]$ , and  $G$  contains the terms in the first-order Taylor's expansion of  $F$  that do not depend on  $\tilde{p}$ . The optimal solution, also called best estimate, is obtained by solving the coupled system

$$(B) \begin{cases} -\frac{\partial \lambda}{\partial r} = F^T \lambda - \sum_{m=1}^M W_{\varepsilon, mm} (\tilde{p}(r_m, z_m) - y_m) \\ \quad \times \delta(r - r_m) \delta(z - z_m), \\ \lambda(R, z) = 0, \end{cases} \tag{B2}$$

$$(A) \begin{cases} \frac{\partial \tilde{p}}{\partial r} = F \tilde{p} + G + C_f \cdot \lambda, \\ \tilde{p}(r=0) = I(z) + C_i \circ \lambda(0, z). \end{cases} \tag{B3}$$

The representer method attempts to uncouple this system by introducing representer functions  $q_m(r, z)$ ,  $1 \leq m \leq M$ , and expressing the solution of the linearized EL system as

$$\tilde{p}(r, z) = p_b(r, z) + \sum_{m=1}^M \gamma_m q_m(r, z), \tag{B4}$$

where  $p_b(r, z)$  is the solution of the error-free model

$$\begin{cases} \frac{\partial p_b}{\partial r} = F p_b + G, \\ p_b(r=0) = I(z), \end{cases} \tag{B5}$$

$\gamma_m$  are the representer coefficients, and the representer functions  $q_m(r, z)$  [and their associated adjoint representer functions  $\mu_m(r, z)$ ] are the solutions of

$$(B_m) \begin{cases} -\frac{\partial \mu_m}{\partial r} = F^T \mu_m - \delta(r - r_m) \delta(z - z_m), \\ \mu_m(R) = 0, \end{cases} \tag{B6}$$

and

$$\begin{cases} \frac{\partial q_m}{\partial r} = F q_m + C_f \cdot \mu_m, \\ q_m(r=0) = C_i \circ \mu_m(0, z). \end{cases} \tag{B7}$$

Let us denote the differential operator  $D = \partial/\partial r - F$ , and omit the dependence on  $(r, z)$  for the sake of clarity. It may be shown that the transpose of  $D$  is the operator  $D^T = -\partial/\partial r - F^T$ . From Eqs. (B4), (B5), and (B7) we get

$$D\tilde{p} = Dp_b + \sum_{m=1}^M \gamma_m Dq_m = G + C_f \sum_{m=1}^M \gamma_m \mu_m. \quad (\text{B8})$$

By the definition of the weighted residual (12) we have

$$\lambda = W_f \cdot (D\tilde{p} - G) = \sum_{m=1}^M \gamma_m \mu_m. \quad (\text{B9})$$

Applying the operator  $D^T$  on Eq. (B9) and using the first equation of Eq. (B2),

$$\begin{aligned} D^T \lambda &= \sum_{m=1}^M \gamma_m D^T \mu_m = -\sum_{m=1}^M \gamma_m \delta(r - r_m) \delta(z - z_m) \\ &= -\sum_{m=1}^M W_{\varepsilon, mm} (\tilde{p}(r_m, z_m) - y_m) \\ &\quad \times \delta(r - r_m) \delta(z - z_m). \end{aligned} \quad (\text{B10})$$

Equating the coefficients of the Dirac functions in Eq. (B10) yields the optimal choice of the representer coefficients

$$\gamma_m = W_{\varepsilon, mm} (\tilde{p}(r_m, z_m) - y_m), \quad 1 \leq m \leq M. \quad (\text{B11})$$

Substituting Eq. (B4) into Eq. (B11) gives

$$\begin{aligned} \gamma_m &= W_{\varepsilon, mm} \left( p_b(r_m, z_m) + \sum_{l=1}^M \gamma_l q_l(r_m, z_m) - y_m \right) \\ &= W_{\varepsilon, mm} \left( p_{bm} + \sum_{l=1}^M \gamma_l q_{lm} - y_m \right), \end{aligned} \quad (\text{B12})$$

and through some rearranging of Eq. (B12) we obtain the linear system

$$\sum_{l=1}^M (q_l^m + W_{\varepsilon, mm}^{-1} \delta_{lm}) \beta_l = y_m - p_{bm}^m, \quad 1 \leq m \leq M, \quad (\text{B13})$$

where  $\delta_{lm}$  is the Kronecker delta. In matrix notation, the  $M$  equations in Eq. (B13) for the representer coefficients  $\gamma_m$  are

$$(Q + C_\varepsilon) \gamma = y - Hp_b, \quad (\text{B14})$$

where  $H$  is the operator that transforms the solution  $p_b$  into the vector of components  $p_{bm} = p_b(r_m, z_m)$ ,  $1 \leq m \leq M$ , and  $W_\varepsilon$  had been defined as the inverse of  $C_\varepsilon$ . Note the similarity between Eq. (B14) and the same linear system (18). The optimal solution is therefore obtained as

$$\tilde{p}(r, z) = p_p(r, z) + (y - Hp_b)^T (Q + C_\varepsilon)^{-1} q(r, z). \quad (\text{B15})$$

However, Eq. (B15) is only feasible if one can afford the computation and storage of all the representer functions. It is referred to as the direct representer method. In practice it is

not necessary to compute and store all the representer functions. Remember that the adjoint and the forward models in Eq. (B1) are coupled by  $M$  values  $\tilde{p}_m = \tilde{p}(r_m, z_m)$ ,  $1 \leq m \leq M$ . The coupling vector appearing in the right-hand side of the adjoint is actually Eq. (B11). Thus, as long as the linear system (B14) can be solved, the resulting vector or representer coefficients can be substituted in the right-hand side of the adjoint model in Eq. (B2), and the adjoint solution will in turn be substituted in the forward model in Eq. (B3) to obtain the optimal solution. This approach, also called the indirect representer method, avoids the computation and storage of all the representer functions.

- Badran, F., Berrada, M., Brajard, J., Crépon, M., Sorror C., Thiria, S., Hermand J.-P., Meyer, M., Perichon, L., and Asch, M. (2008). "Inversion of satellite ocean colour imagery and geoacoustic characterization of seabed properties: Variational data inversion using a semi-automatic adjoint approach," *J. Mar. Sci.* **69**, 126–136.
- Bennett, A. F. (2002). *Inverse Modeling of the Ocean and Atmosphere* (Cambridge University Press, Cambridge), pp. 1–234.
- Bennett, A. F., Chua, B. S., Harrison, D. E., and McPhaden M. J. (1998). "Generalized inversion of Tropical Atmosphere-Ocean (TAO) data and a coupled model of the tropical Pacific Ocean," *J. Climate* **11**, 1768–1792.
- Bennett, A. F., Chua, B. S., Harrison, D. E., and McPhaden M. J. (2000). "Generalized inversion of Tropical Atmosphere-Ocean (TAO) data and a coupled model of the tropical Pacific Ocean. Part II: the 1995-96 La Nina and 1997-98 El Nino," *J. Climate* **13**, 1768–1792.
- Bennett, A. F., Chua, B. S., and Leslie, L. M. (1996). "Generalized inversion of a global numerical weather prediction model," *Meteor. Atmos. Physics* **60**, 165–178.
- Castor, K., Gerstoft, P., Roux, P., Kuperman, W. A., and McDonald, B. E. (2004). "Long-range propagation of finite-amplitude acoustic waves in an ocean waveguide," *J. Acoust. Soc. Am.* **116**(4), 2004–2010.
- Charpentier, I., and Roux P. (2004). "Mode and wavenumber inversion in shallow water using an adjoint method," *J. Comput. Acoust.* **12**(4), 521–542.
- Chen C.-T., and Millero F. J. (1977). "Sound speed in seawater at high pressures," *J. Acoust. Soc. Am.* **62**, 1129–1135.
- Collins, D. (1989). "A higher-order parabolic equation for wave propagation in an ocean overlying an elastic bottom," *J. Acoust. Soc. Am.* **86**, 1459–1464.
- Collins, M. D. (1993). "A split-step Padé solution for parabolic equation method," *J. Acoust. Soc. Am.* **93**, 1736–1742.
- Collins, M. D. (1994). "Generalization of the split-step Padé solution," *J. Acoust. Soc. Am.* **96**, 382–385.
- Collins, M. D., Cederberg, R. J., King, D. B., and Chin-Bing, S. A. (1996). "Comparison of algorithms for solving parabolic wave equations," *J. Acoust. Soc. Am.* **100**(1), 178–182.
- Colosi, J. A., Flatté S. M., and Bracher C. (1994). "Internal-wave effects on 1000-km oceanic acoustic pulse propagation: Simulation and comparison to experiment," *J. Acoust. Soc. Am.* **96**, 452–468.
- Colosi, J. A., Scheer, E. K., Flatté SM., Cornuelle, B. D., Dzieciuch, M. A., Munk, W. H., Worcester, P. F., Howe, B. M., Mercer, J. A., Spindel, R. C., Metzger, K., Birdsall, T. G., and Baggeroer, A. B. (1999). "Comparisons of measured and predicted acoustic fluctuations for a 3250-km propagation experiment in the eastern North Pacific Ocean," *J. Acoust. Soc. Am.* **105**(6), 3202–3218.
- Elisseff, P., Schmidt, H., and Xu, W. (2002). "Ocean acoustic tomography as a data assimilation problem," *IEEE J. Ocean. Eng.* **27**(2), 275–282.
- Fabre, J. P., Rowley, C., Jacobs, G., Coelho, E., Bishop, C., Hong, X., and Cummings, J. (2008). "Environmental acoustic variability characterization for adaptive sampling," in *NRL Review* (Naval Research Laboratory, Washington, DC), pp. 123–126.
- Helber, R. W., Barron, C. N., Carnes, M. R., and Zingarelli, R. A. (2008). "Evaluating the sonic layer depth relative to the mixed layer depth," *J. Geophys. Res.* **113**, C07033, doi:10.1029/2007JC004595.
- Hermand, J. P., Berrada, M., Meyer, M., and Asch, M. (2006). "Adjoint-based geoacoustic inversion with an uncertain sound speed profile," in



- Proceedings of the Eighth European Conference on Underwater Acoustics*, edited by S. M. Jesus and O. C. Rodriguez, Carvoeiro, Portugal.
- Hursky, P., Porter, M. B., Cornuelle, B. D., Hodgkiss, W. S., and Kuperman, W. A. (2004). "Adjoint modeling for acoustic inversion," *J. Acoust. Soc. Am.* **115**(2), 607–619.
- Lam, F. P., Haley, P. J., Janmaat, J., Lermusiaux, P. F. J., Leslie, W. G., Schouten, M. W., te Raa, L. A., and Rixen, M. (2009). "At-sea real-time coupled four-dimensional oceanographic and acoustic forecasts during Battlespace Preparation 2007," *J. Mar. Syst.* **78**(1), S306–S320.
- Le Gac, J.-C., Stéphan, Y., Asch, M., Helluy, P., and Hermand, J.-P. (2004). "A variational approach for geoacoustic inversion using adjoint modeling of a PE approximation model with nonlocal impedance boundary conditions," in *Theoretical and Computational Acoustics 2003*, edited by A. Tolstoy, Y. Teng, and E. Shang (World Scientific Publishing, Singapore), pp. 254–263.
- Leroy, C. C., Robinson, S. P., and Goldsmith, M. J. (2008). "A new equation for the accurate calculation of sound speed in all oceans," *J. Acoust. Soc. Am.* **124**(5), 2774–2782.
- Li, J. L., Jin, L. L., and Xu, W. (2014). "Inversion of internal wave-perturbed sound-speed field via acoustic data assimilation," *IEEE J. Ocean. Eng.* **39**(3), 407–418.
- Martin, P. (2000). "Description of the Navy Coastal Ocean Model Version 1.0," NRL Report No. NRL/FR/7322-00-9961, Naval Research Laboratory, Stennis Space Center, MS.
- Meyer, M., and Hermand J.-P. (2005). "Optimal nonlocal boundary control of the wide-angle parabolic equation for inversion of a waveguide acoustic field," *J. Acoust. Soc. Am.* **117**(5), 2937–2948.
- Millero, F. J., and Li, X. (1994). "Comments on 'On equations for the speed of sound in seawater' [J. Acoust. Soc. Am. **93**, 255–275 (1993)]," *J. Acoust. Soc. Am.* **95**(5), 2757–2759.
- Ngodock, H., and Carrier, M. (2014). "A 4DVAR system for the Navy Coastal Ocean Model. Part I: System description and assimilation of synthetic Observations in Monterey Bay," *Mon. Weather Rev.* **142**(6), 2085–2107.
- Ngodock, H. E., Chua, B. S., and Bennett, A. F. (2000). "Generalized inversion of a reduced gravity primitive equation ocean model and tropical atmosphere ocean data," *Mon. Wea. Rev.* **128**, 1757–1777.
- Ngodock, H. E., Smith, S. R., and Jacobs, G. A. (2007). "Cycling the representer algorithm for variational data assimilation with a nonlinear reduced gravity ocean model," *Ocean Modell.* **19**, 101–111.
- Ngodock, H. E., Smith, S. R., and Jacobs, G. A. (2009). "Cycling the representer method with nonlinear models," in *Data Assimilation for Atmospheric, Oceanic and Hydrologic Applications*, edited by S. K. Park and L. Xu (Springer, New York), Chap. 17, pp. 321–340.
- Thode, A. (2004). "The derivative of a waveguide acoustic field with respect to a three-dimensional sound speed perturbation," *J. Acoust. Soc. Am.* **115**(6), 2824–2833.
- Thode, A., and Kim, K. (2004). "Multiple-order derivatives of a waveguide acoustic field with respect to sound speed, density, and frequency," *J. Acoust. Soc. Am.* **116**(6), 3370–3383.

# A variational data assimilation system for the range dependent acoustic model using the representer method: Theoretical derivations

Hans Ngodock, Matthew Carrier, Josette Fabre, Robert Zingarelli, and Innocent Souopgui

Citation: [The Journal of the Acoustical Society of America](#) **142**, 186 (2017); doi: 10.1121/1.4989541

View online: <http://dx.doi.org/10.1121/1.4989541>

View Table of Contents: <http://asa.scitation.org/toc/jas/142/1>

Published by the [Acoustical Society of America](#)

---

## Articles you may be interested in

[Iterative range estimation in a sloping-bottom shallow-water waveguide using the generalized array invariant](#)  
The Journal of the Acoustical Society of America **142**, 55 (2017); 10.1121/1.4990670

[Spectral analysis of bistatic scattering from underwater elastic cylinders and spheres](#)  
The Journal of the Acoustical Society of America **142**, 110 (2017); 10.1121/1.4990690

[Sound source localization identification accuracy: Envelope dependencies](#)  
The Journal of the Acoustical Society of America **142**, 173 (2017); 10.1121/1.4990656

[Radiation damping of, and scattering from, an arbitrarily shaped bubble](#)  
The Journal of the Acoustical Society of America **142**, 160 (2017); 10.1121/1.4985137

[Diffuse ultrasonic backscatter using a multi-Gaussian beam model](#)  
The Journal of the Acoustical Society of America **142**, 195 (2017); 10.1121/1.4989549

[Sound radiation from impact-driven raked piles](#)  
The Journal of the Acoustical Society of America **142**, 1 (2017); 10.1121/1.4990021

---